

2015

Few-layer titanium trisulfide (TiS_3) field-effect transistors

Alexey Lipatov

University of Nebraska-Lincoln, alipatov@unl.edu

Peter M. Wilson

University of Nebraska – Lincoln

Mikhail Shekhirev

University of Nebraska – Lincoln

Jacob D. Teeter

University of Nebraska – Lincoln

Ross Netusil

University of Nebraska – Lincoln

See next page for additional authors

Follow this and additional works at: <https://digitalcommons.unl.edu/chemfacpub>

 Part of the [Analytical Chemistry Commons](#), [Medicinal-Pharmaceutical Chemistry Commons](#), and the [Other Chemistry Commons](#)

Lipatov, Alexey; Wilson, Peter M.; Shekhirev, Mikhail; Teeter, Jacob D.; Netusil, Ross; and Sinitskii, Alexander, "Few-layer titanium trisulfide (TiS_3) field-effect transistors" (2015). *Faculty Publications -- Chemistry Department*. 90.

<https://digitalcommons.unl.edu/chemfacpub/90>

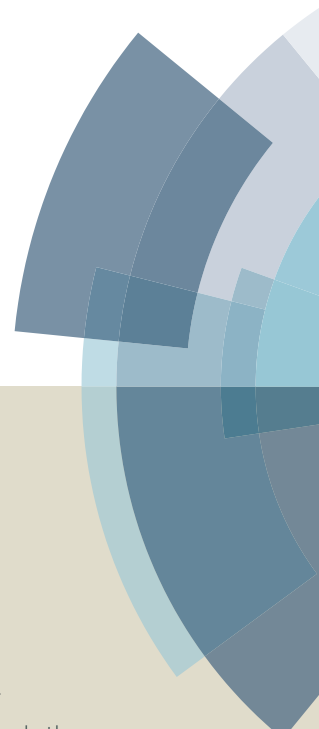
This Article is brought to you for free and open access by the Published Research - Department of Chemistry at DigitalCommons@University of Nebraska - Lincoln. It has been accepted for inclusion in Faculty Publications -- Chemistry Department by an authorized administrator of DigitalCommons@University of Nebraska - Lincoln.

Authors

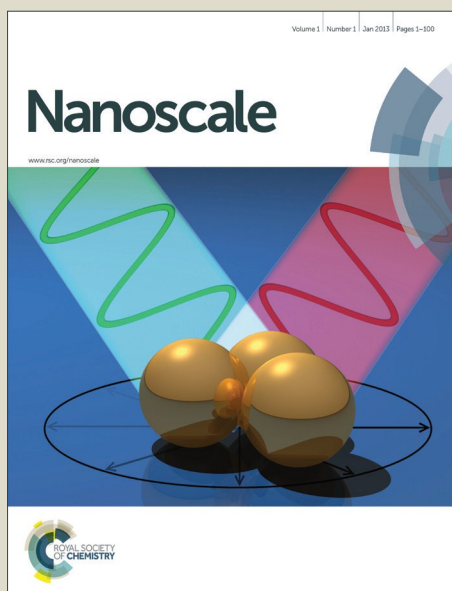
Alexey Lipatov, Peter M. Wilson, Mikhail Shekhirev, Jacob D. Teeter, Ross Netusil, and Alexander Sinitskii

Nanoscale

Accepted Manuscript



This article can be cited before page numbers have been issued, to do this please use: A. Lipatov, P. Wilson, M. Shekhirev, J. Teeter, R. Netusil and A. Sinitskii, *Nanoscale*, 2015, DOI: 10.1039/C5NR01895A.



This is an *Accepted Manuscript*, which has been through the Royal Society of Chemistry peer review process and has been accepted for publication.

Accepted Manuscripts are published online shortly after acceptance, before technical editing, formatting and proof reading. Using this free service, authors can make their results available to the community, in citable form, before we publish the edited article. We will replace this *Accepted Manuscript* with the edited and formatted *Advance Article* as soon as it is available.

You can find more information about *Accepted Manuscripts* in the [Information for Authors](#).

Please note that technical editing may introduce minor changes to the text and/or graphics, which may alter content. The journal's standard [Terms & Conditions](#) and the [Ethical guidelines](#) still apply. In no event shall the Royal Society of Chemistry be held responsible for any errors or omissions in this *Accepted Manuscript* or any consequences arising from the use of any information it contains.

COMMUNICATION

Few-layer titanium trisulfide (TiS₃) field-effect transistors[†]

Cite this: DOI: 10.1039/x0xx00000x

Alexey Lipatov,^a Peter M. Wilson,^a Mikhail Shekhirev,^a Jacob D. Teeter,^a Ross Netusil,^a and Alexander Sinitiskii^{*a,b}Received 00th January 2015,
Accepted 00th January 2015

DOI: 10.1039/x0xx00000x

www.rsc.org/

Titanium trisulfide (TiS₃) is a promising layered semiconductor material. Several-mm-long TiS₃ whiskers can be conveniently grown by the direct reaction of titanium and sulfur. In this study, we exfoliated these whiskers using the adhesive tape approach and fabricated few-layer TiS₃ field-effect transistors (FETs). The TiS₃ FETs showed an n-type electronic transport with room-temperature field-effect mobilities of 18–24 cm²V^{−1}s^{−1} and ON/OFF ratios up to 300. We demonstrate that TiS₃ is compatible with the conventional atomic layer deposition (ALD) procedure for Al₂O₃. ALD of alumina on TiS₃ FETs resulted in mobility increase up to 43 cm²V^{−1}s^{−1}, ON/OFF ratios up to 7000, and much improved subthreshold swing characteristics. This study shows that TiS₃ is a competitive electronic material in the family of two-dimensional (2D) transition metal chalcogenides and can be considered for emerging device applications.

Recently discovered remarkable properties of graphene stimulated interest in other two-dimensional (2D) atomic crystals.^{1–3} Many of the actively studied 2D materials belong to the family of transition metal chalcogenides (TMCs).^{4–6} A large number of TMCs in bulk form have a layered structure with weak interlayer van der Waals interactions.^{2–6} The layers of TMCs can be exfoliated by different approaches to produce mono- and few-layer sheets that can be used for electrical and optical measurements.^{1–7} So far, the experimental studies have mostly focused on TMCs with MX₂ composition (M = Mo, W; X is a chalcogen), such as MoS₂, MoSe₂, WS₂ and WSe₂.^{4,5} However, the TMC family is very rich and contains many other layered materials with interesting properties that received limited attention from the researchers.^{8,9}

One of such TMC materials is titanium trisulfide (TiS₃). In the bulk form, TiS₃ has been studied for several decades.^{10–23} It was shown that millimeter-long whiskers of TiS₃ can be synthesized by a direct reaction of metallic titanium and elemental sulfur in evacuated ampules at 500–600 °C.^{11, 12, 15, 18, 22–24} These whiskers were used for physical property measurements,^{10, 12, 15, 17, 18, 22, 23} which revealed that bulk TiS₃ is a n-type semiconductor with an energy bandgap of

about 1 eV,^{10, 12, 17, 22, 23} and a room-temperature Hall mobility of about 30 cm²V^{−1}s^{−1}.¹⁸

While previous studies have mostly focused on the bulk properties of TiS₃, the introduction and extensive use of the micromechanical exfoliation approach¹ have opened a possibility of accessing properties of monolayer and few-layer TiS₃ flakes. According to the recent theoretical study,²⁵ in a certain crystallographic direction a monolayer of TiS₃ is expected to have higher electron mobility than a single layer of MoS₂. An experimental attempt to exfoliate TiS₃ whiskers into few-layer nanoribbons and study their electronic and optoelectronic properties was reported by Island *et al.*⁹ TiS₃ nanoribbons were shown to have high photoresponse and fast switching times, which makes nanostructured TiS₃ a promising material for applications in optoelectronics and photovoltaics.⁹ However, the room-temperature charge carrier mobilities reported for the set of field-effect transistors (FETs) based on few-layer TiS₃ nanoribbons did not exceed 2.6 cm²V^{−1}s^{−1},⁹ while comparable bottom-gated FETs based on trilayer and thicker MoS₂, the most studied 2D TMC material, exhibit significantly higher mobilities of 10–20 cm²V^{−1}s^{−1},^{26, 27} and reach up to 27 cm²V^{−1}s^{−1} in devices with optimized contact resistances.²⁸ Therefore, in order to demonstrate that TiS₃ is a competitive TMC material for electronics applications, it is necessary to improve its field-effect mobility by at least an order of magnitude.

In this study, we report bottom-gated FETs based on few-layer TiS₃ nanoribbons that have room-temperature field-effect mobilities of 18–23 cm²V^{−1}s^{−1}. Furthermore, according to theory, charge carrier mobilities of 2D semiconductor nanostructures can be significantly improved by modifying their dielectric environment.^{29, 30} Previously, the dielectric screening approach has been successfully applied to graphene^{30, 31} and MoS₂.^{32–35} Here we demonstrate the validity of this approach for the mobility improvement in few-layer TiS₃ FETs by coating the devices with a thin layer of a high-κ dielectric, Al₂O₃, which results in measured field-effect mobilities up to 43 cm²V^{−1}s^{−1} as well as much improved subthreshold swing (S) characteristics. These results demonstrate that TiS₃ is a competitive electronic material in the 2D TMC family and can be considered for emerging device applications.^{3, 4, 6}



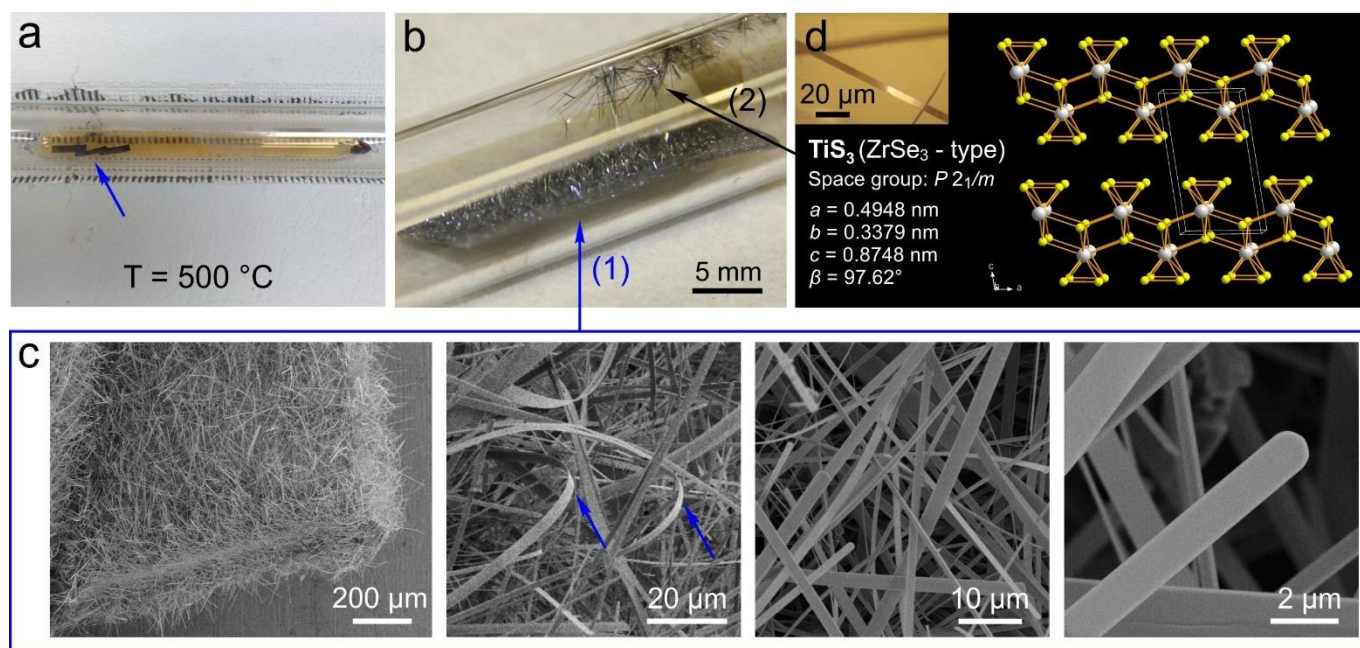


Fig. 1 Synthesis and characterization of TiS_3 whiskers. (a) Optical photograph of the reaction ampule during the synthesis. The ampule is filled with the orange-brown sulphur vapour. The arrow shows three pieces of Ti foil. (b) Optical photograph of the reaction ampule after the synthesis. Arrows show (1) a piece of Ti foil covered with a forest of TiS_3 whiskers and (2) larger TiS_3 whiskers that have grown on the surface of quartz. (c) SEM images of TiS_3 whiskers grown on Ti foil, see (1) in panel (b), at different magnifications. The arrows in the second panel show bent TiS_3 whiskers. (d) Crystal structure of TiS_3 with the lattice parameters. Inset: optical photograph of one of the TiS_3 whiskers shown by the arrow (2) in panel (b).

Following previous studies, we have grown TiS_3 whiskers via the direct reaction of titanium and sulfur.^{11, 12, 15, 18, 24} In a typical synthesis, ~0.1 g piece of a 0.25-mm-thick Ti foil and ~0.2 g of S are sealed in evacuated ($p \sim 200$ mTorr) quartz ampule. The ampule is placed in a tube furnace, where it is heated up to 500 °C and annealed for 3 days. During the reaction sulfur exists in a gas phase, as can be seen by the orange-brown vapor inside the ampule (Figure 1a); three pieces of Ti foil are indicated by the blue arrow. Figure 1b demonstrates the optical photograph of the reaction ampule after the synthesis. The arrow (1) shows one of the pieces of Ti foil; it is covered by dense forest of TiS_3 whiskers that are typically 100–200 μm long. Interestingly, the whiskers grow not only on Ti foil, but also on the surface of quartz ampule, as shown by the arrow (2) in Figure 1b. These whiskers generally grow longer than the whiskers on Ti foil and often exceed 5 mm in length after 3 days of growth. At the end of the synthesis the ampule is moved from the center of the furnace to create a ~ 100 °C temperature gradient, such that the end of the ampule containing the pieces of Ti foil remains at ~ 500 °C while the opposite end of the ampule is cooled below the boiling point of sulfur (444.7 °C). As a result, TiS_3 whiskers are cleaned from unreacted sulfur, which condenses in the cold end of the ampule. One hour later the ampule is cooled down to room temperature and TiS_3 whiskers are collected for materials characterization and electrical measurements.

Figure 1c shows scanning electron microscopy (SEM) images at different magnifications of the TiS_3 whiskers grown on a Ti substrate. These whiskers have a shape of thin ribbons that are typically over 100 μm long, a few μm wide and less than half a micrometer thick; these dimensions are in accord with previously reported observations for similarly prepared samples.^{9, 22} The ribbon shape of TiS_3 whiskers is illustrated by the second panel in Figure 1c, which shows several bent whiskers (two of them are indicated by the blue arrows). Additional SEM data for TiS_3 whiskers grown on a Ti substrate is provided in Figure S1. Based on the data presented in

Figure 1c, S1a and similar SEM images we prepared a width distribution of TiS_3 whiskers, which is shown in Figure S1b. The size distribution is quite broad with a maximum at $w \sim 7$ μm ; a substantial number of whiskers are wider than 20 μm . TiS_3 whiskers were also characterized by Raman spectroscopy; the results presented in Figure S2 are in agreement with the previously reported data.³⁶

For the device fabrication and electrical measurements we used TiS_3 whiskers grown on quartz (see the arrow (2) in Figure 1b), which were easier to handle because of their larger size. The inset in Figure 1d shows the optical microscopy image of one these larger TiS_3 whiskers, which had a length of about 0.6 mm and a width of about 8 μm . This whisker was studied by the single-crystal X-ray diffraction (XRD). A single crystal had a monoclinic symmetry with the space group $P2_1/m$ and lattice parameters $a = 0.4948(7)$, $b = 0.3379(5)$, $c = 0.8748(12)$ nm, and $\beta = 97.62(2)^\circ$. Direct methods yielded a completely ordered atom arrangement isotopic with the structure type of ZrSe_3 ;³⁷ the results of XRD measurements are summarized in Tables S1 and S2 in Supplementary Information. The crystal structure of TiS_3 can be described as a stack of 2D layers formed by one-dimensional (1D) chains of TiS_3 prisms, see Figure 1d. TiS_3 can be viewed as $\text{Ti}^{4+}\text{S}_2^{2-}$, containing both sulfide and disulfide units; these units form trigonal prisms with Ti^{4+} centers.

For the device fabrication, one of the TiS_3 whiskers grown on quartz surface was mechanically exfoliated using adhesive tape¹ and transferred to a p-type silicon substrate covered with a 300-nm-thick layer of SiO_2 (SQI). Because of the quasi-1D structure of TiS_3 , the whiskers do not only exfoliate into 2D sheets but also break longitudinally along the b axis, resulting in thin TiS_3 nanoribbons that are much narrower than the original whiskers. Few-layer TiS_3 nanoribbons with thicknesses of 9–11 nm were found on the surface of a Si/SiO_2 substrate by optical microscopy. Electronic devices with few-layer TiS_3 nanoribbons bridging Cr/Au (3 nm/20 nm) electrodes



were fabricated by standard electron-beam lithography followed by electron-beam evaporation; the details of the device fabrication and materials characterization could be found in Supplementary Information. The schematic of a typical TiS_3 -based device with Cr/Au source (S) and drain (D) electrodes on a p^{++} -Si/SiO₂ substrate (the heavily doped p-type silicon was used as the back gate electrode, G) is shown in Figure 2a.

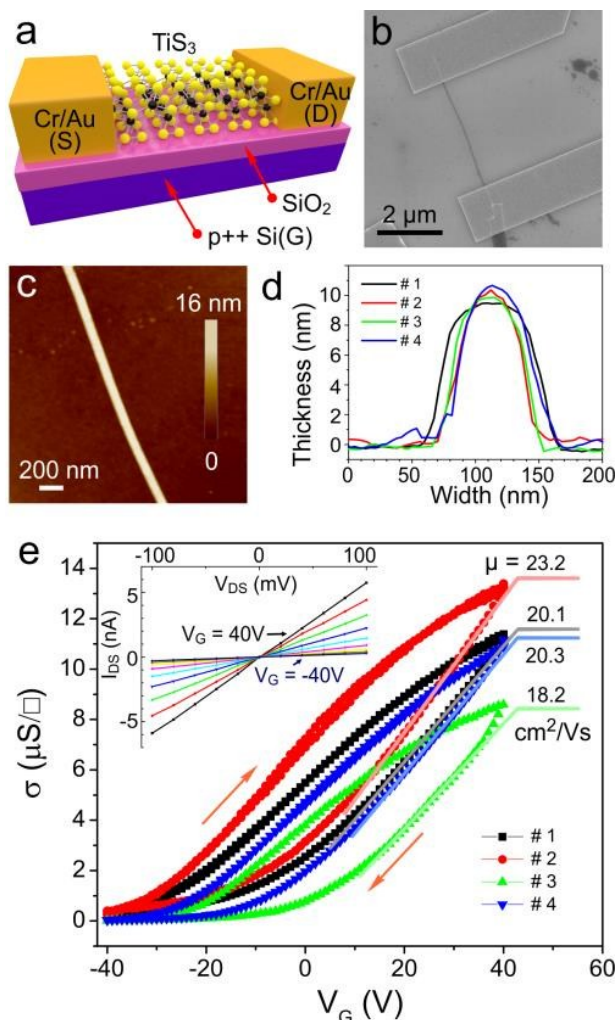


Fig. 2 Few-layer TiS_3 FETs. (a) Scheme of a TiS_3 -based device on a Si/SiO₂ substrate; see text for details. (b) SEM image of a typical TiS_3 FET. Dark strip in the image is a TiS_3 nanoribbon that connects two Cr/Au electrodes. (c) Atomic force microscopy (AFM) image of the fragment of the TiS_3 nanoribbon shown in (b). (d) Representative height profiles measured across the TiS_3 nanoribbon shown in (c), see device #1, and three other TiS_3 nanoribbons used in this study; see text for details. (e) Conductivity (σ) – gate voltage (V_G) dependencies for all four TiS_3 FETs measured in this study. $V_{DS} = 0.1$ V. The mobility (μ) values are extracted from the linear regions (solid lines) in these dependencies. The inset shows drain-source current (I_{DS}) – drain-source voltage (V_{DS}) dependencies for the device shown in panel (b) (device #1) measured at different V_G ranging from -40 to 40 V with a 10 V step.

Figure 2b shows the SEM image of one of the four TiS_3 FETs that were fabricated and tested in this study; SEM and AFM images of other devices are shown in Figure S3 in Supplementary Information. Figure 2c shows the AFM image of the central portion of the TiS_3 nanoribbon channel of the device. The height profile measured across this TiS_3 nanoribbon shows a step of ~ 9.5 nm; see the black line in Figure 2d. For comparison, we also show height profiles measured for other three devices (Figure 2d) to demonstrate that all

TiS_3 nanoribbons measured in this work had comparable thicknesses.

Electrical measurements of TiS_3 FETs were performed in vacuum ($p \sim 1 \times 10^{-6}$ Torr). Prior to the measurements the devices were evacuated for ~ 24 h to minimize the effect of surface adsorbates.³⁸ Figure 2e shows that all four TiS_3 devices exhibited very similar electronic behavior. For all devices the drain-source current (I_{DS}) – drain-source voltage (V_{DS}) dependencies at different gate voltages (V_G) were linear, indicating Ohmic contacts between TiS_3 nanoribbons and Cr/Au electrodes; a representative set of data for one of the TiS_3 FETs is shown in the inset in Figure 2e. This figure also shows conductivity (σ) – gate voltage (V_G) dependencies for all devices, demonstrating the electronic behavior typical for FETs with n-type channels. These dependencies are also hysteretic, which is likely caused by the charge traps at the SiO₂/ TiS_3 interface similar to SiO₂/MoS₂.²⁷ From the linear regions in the $\sigma - V_G$ dependencies we estimate that the few-layer TiS_3 FETs have field-effect mobilities of $18\text{--}23 \text{ cm}^2\text{V}^{-1}\text{s}^{-1}$, which is comparable with the mobilities reported for few-layer MoS₂ devices.^{26–28} The ON/OFF ratios defined as the ratios of the largest and smallest I_{DS} values in V_G dependencies were in the range of 30–300.

The conductivities presented in Fig. 2e were measured using a two-contact method and therefore include a contribution from the contact resistances. In order to evaluate the intrinsic electronic properties of exfoliated TiS_3 whiskers we fabricated and tested two multiterminal devices and used them for four-point probe conductivity measurements, see Figures S4 and S5 and associated comments in Supplementary Information. The field-effect mobilities measured for multiterminal TiS_3 devices using a four-point probe method to exclude the contact resistance contribution were 21.1 and $24.2 \text{ cm}^2\text{V}^{-1}\text{s}^{-1}$. These values are in a great agreement with the mobilities measured for two-terminal devices (Figure 2e). While a more detailed investigation of contact resistance effects could be a subject of a separate study,³⁹ our results show that contact resistances appear to not have a dominant effect on the electronic characteristics of TiS_3 FETs.

As we indicated earlier, dielectric screening is a very effective approach to improve charge carrier mobilities of 2D semiconductor nanostructures.^{29–35} In order to demonstrate the effectiveness of this approach for the mobility enhancement in few-layer TiS_3 FETs, we used atomic layer deposition (ALD) to coat the devices with a 30 nm layer of Al₂O₃. Trimethylaluminum and water were used as Al₂O₃ precursors; additional details on ALD are given in Supplementary Information. Since TiS_3 has not been long considered as a material for electronics, nothing has been reported so far about its compatibility with conventional ALD procedures. For example, preparation of uniform dielectric layers on graphene has proved to be a challenge,^{40–42} as graphene has no functional groups, which hinders the surface modification with common ALD precursors (the direct ALD of Al₂O₃ using the same precursors results in oxide nucleation only at the edges of graphene).⁴⁰ In contrast, the standard ALD procedure for Al₂O₃ growth worked well for TiS_3 . Figure 3a,b shows the same area of a TiS_3 nanoribbon channel of one of the devices before and after ALD of Al₂O₃, respectively. In the process, the color of the Si/SiO₂ substrate changed from purple to green. However, on the nanoscale the morphology of the TiS_3 nanoribbon and the substrate barely changed, suggesting a very uniform growth of Al₂O₃ by ALD (Figure 3a,b). This conclusion is further confirmed by the representative height profiles shown in Figure 3c. Before ALD of Al₂O₃ the height profile measured across the TiS_3 nanoribbon along the yellow line in Figure 3a showed a step height of about 10 nm. After the growth of 30 nm of Al₂O₃ the height profile measured in the same place is nearly the same, suggesting that alumina layers of comparable thicknesses have grown on the



COMMUNICATION

TiS₃ and Si/SiO₂ substrate. Thus, this work demonstrates the compatibility of TiS₃ with conventional ALD procedures, which is important for the future studies of TiS₃ electronic devices.

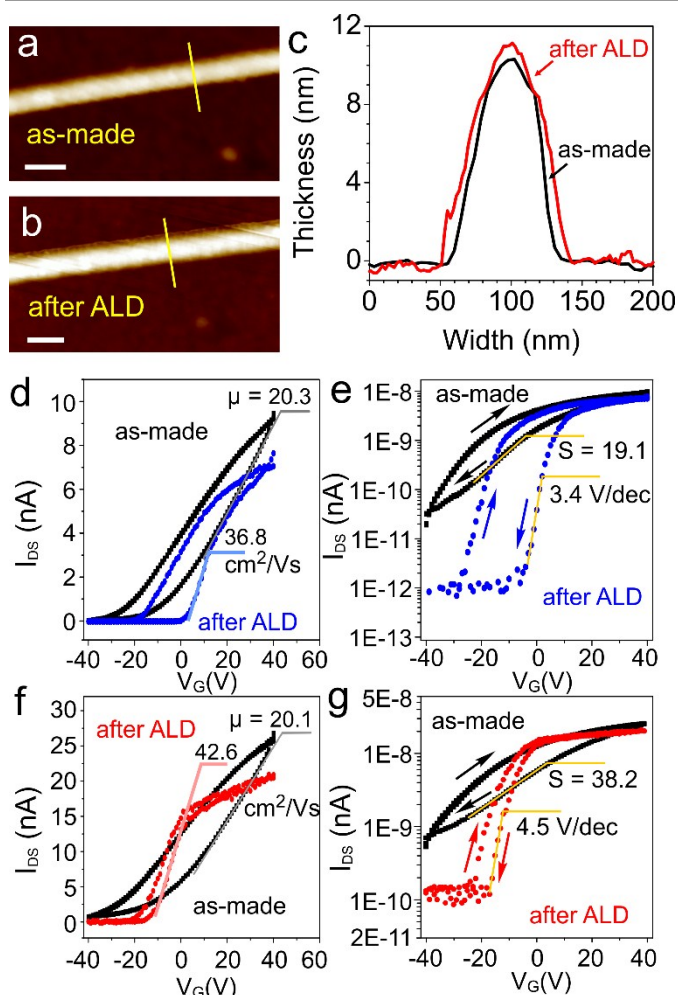


Fig. 3 ALD of Al₂O₃ on TiS₃ FETs. (a) AFM image of a fragment of TiS₃ nanoribbon channel of a device. (b) AFM image of the same area as in (a) after ALD of 30 nm of Al₂O₃. Scale bars in (a,b) are 100 nm. (c) Height profiles measured across the TiS₃ nanoribbon along the yellow lines in (a) and (b). (d,e) Comparison of the drain-source current (I_{DS}) – gate voltage (V_G) dependencies for the same device (# 4) before and after ALD of Al₂O₃ shown in (d) linear and (e) semi-logarithmic coordinates. $V_{DS} = 0.1$ V. (f,g) Comparison of the drain-source current (I_{DS}) – gate voltage (V_G) dependencies for another device (# 1) before and after ALD of Al₂O₃ shown in (f) linear and (g) semi-logarithmic coordinates. $V_{DS} = 0.1$ V.

Figure 3d-g shows $I_{DS} - V_G$ dependencies in linear and semi-logarithmic coordinates for two TiS₃ FETs before and after ALD of Al₂O₃; other devices showed similar behavior. These $I_{DS} - V_G$ plots show that Al₂O₃ deposition may have different effects on the hysteresis of electronic transport observed in alumina-coated TiS₃ FETs. The Al₂O₃-coated device shown in Figure 3d,e exhibits a considerable hysteresis, while in the other Al₂O₃-coated FET (Figure 3f,g) the hysteresis visibly shrinks compared to the as-made TiS₃ FET before Al₂O₃ ALD. As in the case of as-made TiS₃ FETs we attribute this hysteretic behavior to the interfacial charge trapping.²⁷ While we do not investigate this effect in detail, it is interesting to note that the alumina or another high- κ dielectric layer on top of TiS₃ may provide another interface for the charge-trap engineering. The data presented in Figure 3d-g suggest that with a proper optimization of the deposition procedure it may be possible to either

minimize the hysteretic behavior of TiS₃ FETs or create devices with large $\sigma - V_G$ hysteresis loops, which may be of interest, for example, for memory applications.⁴³ The optimization of the ALD procedure using high- κ dielectrics not limited to Al₂O₃ will be the subject of our future studies.

Other than the different features in the shape of $I_{DS} - V_G$ hysteresis loops, the effect of Al₂O₃ deposition on the electronic properties of TiS₃ devices was quite consistent. Figure 3d-g shows that the Al₂O₃ deposition has an overall positive effect on the electronic properties of TiS₃ FETs. For the TiS₃ FET shown in Figure 3d the dielectric screening resulted in the field-effect mobility improvement from 20.3 to 36.8 cm²V⁻¹s⁻¹, and for the other device the mobility improved from 20.1 to 42.6 cm²V⁻¹s⁻¹ (Figure 3f). Interestingly, the Al₂O₃ ALD also improved the ON/OFF ratios of TiS₃ FETs, which can be seen in logarithmic I_{DS} coordinates (Figure 3e,g). For the device shown in Figure 3e, the ON/OFF ratio improved from 300 to 7100, and for the other device (Figure 3g) it improved from 40 to 170. The other two Al₂O₃-coated TiS₃ FETs exhibited ON/OFF ratios of 155 and 180. Positive effect of alumina ALD on the device characteristics of TiS₃ FETs can be further illustrated by the subthreshold swing (S) change. As can be seen in Figures 3e,g and S6, the as-prepared TiS₃ FETs had S values ranging from 19.1 to 44.3 V/dec; after Al₂O₃ ALD the S values decreased to 3.4-4.8 V/dec; the S values for all four devices before and after alumina ALD are summarized in Figure S6c. With these device properties TiS₃ appears to be a promising electronic material that can be positively compared with other more intensively studied members of the 2D TMC family.⁴

In summary, we have fabricated few-layer TiS₃ FETs and tested their electronic properties. The TiS₃ FETs showed an n-type electronic transport with room-temperature field-effect mobilities of 18-24 cm²V⁻¹s⁻¹ and ON/OFF ratios up to 300. We also demonstrate that TiS₃ is compatible with the conventional ALD procedure for Al₂O₃. ALD of alumina on TiS₃ FETs resulted in mobility improvement up to 43 cm²V⁻¹s⁻¹ and ON/OFF ratios of up to ~7000; S values after Al₂O₃ ALD decreased from 19.1-44.3 to 3.4-4.8 V/dec. This study shows that TiS₃ is a promising 2D TMC material that can be further explored in the future device studies.

Acknowledgments

This work was supported by the National Science Foundation (NSF) through the Nebraska Materials Research Science and Engineering Center (MRSEC) (grant No. DMR-1420645). The ALD equipment is a part of the Center for Nanohybrid Functional Materials (CNFM) facilities supported by the NSF EPSCoR (grant No. EPS-1004094). This research was performed in part in Central Facilities of the Nebraska Center for Materials and Nanoscience (NCMN), which is supported by the Nebraska Research Initiative. We thank Prof. Xiao Cheng Zeng (ref.25) for drawing our attention to the 2D TiS₃ material.

Notes and references

- ^a Department of Chemistry, University of Nebraska – Lincoln, Lincoln, NE 68588, USA E-mail: sinitskii@unl.edu
- ^b Nebraska Center for Materials and Nanoscience, University of Nebraska – Lincoln, Lincoln, NE 68588, USA
- [†] Electronic Supplementary Information (ESI) available: Experimental details (synthesis and characterization). See DOI: 10.1039/c000000x/

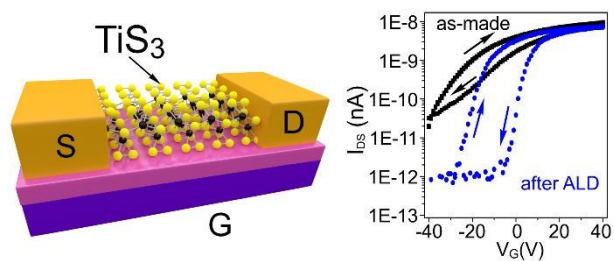
- 1 K. S. Novoselov, D. Jiang, F. Schedin, T. J. Booth, V. V. Khotkevich, S. V. Morozov and A. K. Geim, *Proc. Natl. Acad. Sci. U. S. A.*, 2005, **102**, 10451-10453.



- 2 A. K. Geim and I. V. Grigorieva, *Nature*, 2013, **499**, 419-425.
- 3 S. Z. Butler, S. M. Hollen, L. Cao, Y. Cui, J. A. Gupta, H. R. Gutiérrez, T. F. Heinz, S. S. Hong, J. Huang, A. F. Ismach, E. Johnston-Halperin, M. Kuno, V. V. Plashnitsa, R. D. Robinson, R. S. Ruoff, S. Salahuddin, J. Shan, L. Shi, M. G. Spencer, M. Terrones, W. Windl and J. E. Goldberger, *ACS Nano*, 2013, **7**, 2898-2926.
- 4 Q. H. Wang, K. Kalantar-Zadeh, A. Kis, J. N. Coleman and M. S. Strano, *Nat Nano*, 2012, **7**, 699-712.
- 5 M. Chhowalla, H. S. Shin, G. Eda, L.-J. Li, K. P. Loh and H. Zhang, *Nat Chem*, 2013, **5**, 263-275.
- 6 D. Jariwala, V. K. Sangwan, L. J. Lauhon, T. J. Marks and M. C. Hersam, *ACS Nano*, 2014, **8**, 1102-1120.
- 7 G. Cunningham, M. Lotya, C. S. Cucinotta, S. Sanvito, S. D. Bergin, R. Menzel, M. S. P. Shaffer and J. N. Coleman, *ACS Nano*, 2012, **6**, 3468-3480.
- 8 Y. Huang, E. Sutter, J. T. Sadowski, M. Cotlet, O. L. A. Monti, D. A. Racke, M. R. Neupane, D. Wickramaratne, R. K. Lake, B. A. Parkinson and P. Sutter, *ACS Nano*, 2014, **8**, 10743-10755.
- 9 J. O. Island, M. Buscema, M. Barawi, J. M. Clamagirand, J. R. Ares, C. Sánchez, I. J. Ferrer, G. A. Steele, H. S. J. van der Zant and A. Castellanos-Gomez, *Advanced Optical Materials*, 2014, **2**, 641-645.
- 10 H. G. Grimmeiss, A. Rabenau, H. Hahn and P. Ness, *Z. Elektrochem.*, 1961, **65**, 776-783.
- 11 H. Haraldsen, E. Rost, A. Kjekshus and Steffens, *Acta Chem. Scand.*, 1963, **17**, 1283-&.
- 12 L. Brattas and A. Kjekshus, *Acta Chem. Scand.*, 1972, **26**, 3441-3449.
- 13 S. Furuseth, L. Brattas and A. Kjekshus, *Acta Chemica Scandinavica A*, 1975, **29**, 623-631.
- 14 D. W. Murphy and F. A. Trumbore, *J. Electrochem. Soc.*, 1976, **123**, 960-964.
- 15 S. Kikkawa, M. Koizumi, S. Yamanaka, Y. Onuki and S. Tanuma, *physica status solidi (a)*, 1980, **61**, K55-K57.
- 16 P.-L. Hsieh, C. M. Jackson and G. Grüner, *Solid State Commun.*, 1983, **46**, 505-507.
- 17 O. Gorochov, A. Katty, N. Lenagard, C. Levyclement and D. M. Schleich, *Mater. Res. Bull.*, 1983, **18**, 111-118.
- 18 E. Finkman and B. Fisher, *Solid State Commun.*, 1984, **50**, 25-28.
- 19 I. G. Gorlova and V. Y. Pokrovskii, *Jetp Lett.*, 2009, **90**, 295-298.
- 20 I. G. Gorlova, V. Y. Pokrovskii, S. G. Zybtev, A. N. Titov and V. N. Timofeev, *J. Exp. Theor. Phys.*, 2010, **111**, 298-303.
- 21 I. G. Gorlova, S. G. Zybtev, V. Y. Pokrovskii, N. B. Bolotina, I. A. Verin and A. N. Titov, *Physica B: Condensed Matter*, 2012, **407**, 1707-1710.
- 22 I. J. Ferrer, M. D. Maciá, V. Carcelén, J. R. Ares and C. Sánchez, *Energy Procedia*, 2012, **22**, 48-52.
- 23 I. J. Ferrer, J. R. Ares, J. M. Clamagirand, M. Barawi and C. Sánchez, *Thin Solid Films*, 2013, **535**, 398-401.
- 24 F. Lévy and H. Berger, *Journal of Crystal Growth*, 1983, **61**, 61-68.
- 25 J. Dai and X. C. Zeng, *Angewandte Chemie International Edition*, 2015, DOI: 10.1002/anie.201502107.
- 26 H. Wang, L. Yu, Y.-H. Lee, Y. Shi, A. Hsu, M. L. Chin, L.-J. Li, M. Dubey, J. Kong and T. Palacios, *Nano Lett.*, 2012, **12**, 4674-4680.
- 27 S. Ghatak, A. N. Pal and A. Ghosh, *ACS Nano*, 2011, **5**, 7707-7712.
- 28 J. Kang, W. Liu and K. Banerjee, *Appl. Phys. Lett.*, 2014, **104**, 093106.
- 29 D. Jena and A. Konar, *Phys. Rev. Lett.*, 2007, **98**, 136805.
- 30 C. Jang, S. Adam, J. H. Chen, E. D. Williams, S. Das Sarma and M. S. Fuhrer, *Phys. Rev. Lett.*, 2008, **101**, 146805.
- 31 F. Chen, J. Xia, D. K. Ferry and N. Tao, *Nano Lett.*, 2009, **9**, 2571-2574.
- 32 B. Radisavljevic, A. Radenovic, J. Brivio, V. Giacometti and A. Kis, *Nat Nano*, 2011, **6**, 147-150.
- 33 M. S. Fuhrer and J. Hone, *Nat Nano*, 2013, **8**, 146-147.
- 34 B. Radisavljevic and A. Kis, *Nat Nano*, 2013, **8**, 147-148.
- 35 B. Radisavljevic and A. Kis, *Nat Mater*, 2013, **12**, 815-820.
- 36 D. W. Galliard, W. R. Nieveen and R. D. Kirby, *Solid State Commun.*, 1980, **34**, 37-39.
- 37 S. Furuseth, L. Brattås and A. Kjekshus, *Acta Chem. Scand. A*, 1975, **29a**, 623-631.
- 38 A. Sinitskii, A. Dimiev, D. V. Kosynkin and J. M. Tour, *ACS Nano*, 2010, **4**, 5405-5413.
- 39 F. N. Xia, V. Perebeinos, Y. M. Lin, Y. Q. Wu and P. Avouris, *Nat. Nanotechnol.*, 2011, **6**, 179-184.
- 40 X. Wang, S. M. Tabakman and H. Dai, *J. Am. Chem. Soc.*, 2008, **130**, 8152-8153.
- 41 J. M. P. Alaboson, Q. H. Wang, J. D. Emery, A. L. Lipson, M. J. Bedzyk, J. W. Elam, M. J. Pellin and M. C. Hersam, *ACS Nano*, 2011, **5**, 5223-5232.
- 42 A. Lipatov, B. B. Wymore, A. Fursina, T. H. Vo, A. Sinitskii and J. G. Redepenning, *Chem. Mat.*, 2015, **27**, 157-165.
- 43 J. Yao, Z. Jin, L. Zhong, D. Natelson and J. M. Tour, *ACS Nano*, 2009, **3**, 4122-4126.



Table of contents entry



Titanium trisulfide (TiS_3) whiskers can be mechanically exfoliated and used for fabrication of field-effect transistors, which upon coating with Al_2O_3 exhibit mobilities up to $43\text{ cm}^2\text{V}^{-1}\text{s}^{-1}$ and ON/OFF ratios up to 7000.